Study of the adhesive properties versus stability/aging of hernia repair meshes after deposition of RF activated plasma polymerized acrylic acid coating

UNIVERSITÀ DEGLI STUDI DI TORINO

Study of the adhesive properties versus stability/aging of hernia repair meshes after deposition of RF activated plasma polymerized acrylic acid coating

Paola Rivolo[a], Roberto Nisticò[b,*], Fabrizio Barone[b], Maria Giulia Faga[c], Donatella Duraccio[c], Selanna Martorana[d], Serena Ricciardi[a], Giuliana Magnacca[b]

[a] Politecnico di Torino, Department of Applied Science and Technology, C.so Duca degli Abruzzi 24, 10129 Torino, Italy
[b] University of Torino, Department of Chemistry and NIS Centre, Via P. Giuria 7, 10125 Torino, Italy
[c] CNR-IMAMOTER, Strada delle Cacce 73, 10135 Torino, Italy
[d] Herniamesh S.r.l., Via F.lli Meliga 1/C, 10034 Chivasso, Italy
* Corresponding author. E-mail: roberto.nistico@unito.it, Ph.: +39-011-6707533, Fax: +39-011-6707855

Abstract
In order to confer adhesive properties to commercial polypropylene (PP) meshes, a surface plasma-induced deposition of poly-(acrylic acid) (PPAA) is performed. Once biomaterials were functionalized, different post-deposition treatments (i.e. water washing and/or thermal treatments) were investigated with the aim of monitoring the coating degradation (and therefore the loss of adhesion) after 3 months of aging in both humid/oxidant (air) and inert (nitrogen) atmospheres. A wide physicochemical characterization was carried out in order to evaluate the functionalization effectiveness and the adhesive coating homogeneity by means of static water drop shape analysis and several spectroscopies (namely, FTIR, UV-Visible and X-rays Photoemission Spectroscopy). The modification of the adhesion properties after post-deposition treatments as well as aging under different storage atmospheres were investigated by means of Atomic Force Microscopy (AFM) used in Force/Distance (F/D) mode. This technique confirms itself as a powerful tool for unveiling the surface adhesion capacity as well as the homogeneity of the functional coatings along the fibers. Results obtained evidenced that post-deposition treatments are mandatory in order to remove all oligomers produced during the plasma-treatment, whereas aging tests evidenced that these devices can be simply stored in presence of air for at least three months without a meaningful degradation of the original properties.

Keywords: Adhesive thin coatings; AFM Force/Distance mode; Hernia-repair PP meshes; Plasma polymerization; Surface science.

1. Introduction
The use of polymeric meshes during the hernia-repair surgical operations is a routine procedure [1-4], although still nowadays there are different phenomena which can cause hernioplasty complications, for instance surgical infections or the post-operative prostheses displacement with detachment of the polymeric device, collapse of the anchoring sutures and reformation of the hernia disease [5].
In order to solve these issues, thus reducing the risk related to hernioplasty failure, the surface modification of standard polymeric meshes seems to be a promising route to follow [6]. Among others, plasma treatments have recently gained much attention, thanks to their ability to induce modifications only at the surface level without altering the intrinsic physicochemical and mechanical properties of the prosthetic biomaterial [7-12].
Recently, the plasma deposition technique has been successfully used to functionalize polymeric materials with plasma poly-(acrylic acid) (PPAA) layers for clinical purposes, such as exploiting -COOH groups in covalent binding of c-DNA probes [13] or as substrates for the adhesion of human cells colonies in a non-specific manner [14-15]. Moreover, the adoption of a thin coating, produced by plasma deposition, avoid the lack of the open porosity between the biomaterials fibers necessary for an optimal tissue infiltration and proper mesh integration in the biological tissue [5].

In detail, the plasma polymerization process conditions which guarantee a good compromise between the maintenance of the functional groups (in this case, the carboxylic groups of the polyacrylic acid) and the increase of the coatings mechanical properties (obtained synthesizing highly branched and cross-linked PPAA), can be reached by working following a "monomer-deficient regime", as described by Yasuda *et al*. [16], using a pulsed-plasma deposition in order to obtain a better control of the surface reactivity and the film chemistry [17]. The monomer-deficient domain corresponds to a high input power/gas flow ratio (W/F), based on the following equation:

$$R_m/F = G exp^{(-Ea/(W/F))} \quad \textbf{(Equation 1)}$$

where R_m is the mass deposition rate, F is the total gas flow, G is a constant (which comprises the decomposition rate of the monomer, that strongly depends on the plasma apparatus), E_a is the apparent activation energy, W is the input power and W/F is the average energy per particle [18-20].

However, even though all these precautions have been taken into account, the stability over time and atmospheric conditions of such functional plasma-polymerized thin coatings is still a limiting factor, which significantly reduces the application of these smart devices in the biomedical fields. In this context, the use of atomic force microscopy in force/distance (AFM F/D) mode can be a powerful tool for evaluating both the stability of such adhesive thin coatings and how incorrect post-deposition treatments can dramatically alter the plasma-induced surface properties [21-22].

Therefore, in this paper, we extend our previous work [23], focused on the surface functionalization of polypropylene (PP) meshes by an adhesive thin-coatings made by plasma-polymerized polyacrylic acid (PPAA), considering the effects of post-deposition treatments (i.e. no treatment, water washing and water washing followed by a thermal treatment) and following the coating stability after 3 months of aging in humid/oxidant (air) and inert (nitrogen) atmospheres. Among all the physico-chemical techniques here selected, AFM in F/D mode confirms to be a very useful tool to optimize the post-deposition procedure, making these functional devices suitable for a real and feasible industrial scaling-up.

2. Experimental

2.1 Biomedical devices and reagents

Monofilament PP meshes for surgical applications were provided by Herniamesh® S.r.l. (Chivasso, Italy). Lightweight (ca. 30 g m^{-2}) PP flat rectangular meshes probes were 6 × 11 cm, with 0.32 ± 10 % mm of thickness, and fibers diameter of 80 ± 10 % µm. Other reagents used were: Acrylic acid monomer (AA, $CH_2CH(COOH)$, Sigma Aldrich, purity 99%, CAS 79-10-7), Toluidine Blue O (TBO, $C_{15}H_{16}ClN_3S$, Sigma, Technical Grade purity, CAS 92-31-9), Sodium hydroxide (NaOH, Fluka, purity 97 %, CAS 1310-73-2), and Acetic acid (CH_3COOH, Aldrich, purity 99.7 %, CAS 64-19-7). All chemicals were used without purification.

2.2 Plasma polymerization apparatus and treatment conditions

Plasma-polymerized Poly-(Acrylic-Acid) (PPAA) thin films deposition was performed as previously reported [23]. The samples were introduced in a Plasma Enhanced Chemical Vapor Deposition (PECVD) reactor (Chamber Base Pressure = 3.7 ± 0.2 Pa; Radio frequency RF = 13.56 MHz) equipped with a delivery frame suitable to inject vapors coming from liquid reactants (monomer precursors). The reactor is a cylindrical closed chamber (320 mm wide and 200 mm height) made by stainless steel. Argon was selected as gas-carrier in order to sustain plasma discharge, for all experiments. The complete treatment consists of a two-steps process: i) the surface etching by continuous Ar plasma discharge (for cleaning the fibers surface and promoting the adhesion of the PPAA coating); ii) AA polymerization by pulsed plasma discharge. Surface etching step was performed by flowing Ar gas (flow = 20 sccm), applying a discharge RF power of 50 W, for 5 minutes at a total pressure of 30.7 Pa. Polymerization was performed by admitting acrylic acid vapors (flow = 3 sccm) diluted in Ar (flow = 20 sccm), applying a discharge Radio Frequency (RF)

power of 200 W, a duty cycle of 10% (on time = 10 ms, off time = 90 ms) for 10 minutes at a total pressure of 19.3 Pa. The expected thickness of PPAA layer for the used experimental conditions was of ca. 100 ± 20 nm, measured on a flat surface [13].

PPAA-functionalized samples were treated in two different post-deposition conditions in order to evidence the best preparation procedure: 1) incubation: samples were soaked in deionized water Milli-Q grade (dH_2O) for 30 minutes under oscillating shaking in order to remove unstable surface oligomers formed at the end of the plasma process, 2) incubation and thermal treatment: incubated samples were dried under N_2 flux and heated at 80 °C for 1 hour in oven. These samples were compared with the untreated ones. Moreover, two different storage atmospheres were tested: inert (nitrogen) and humid/oxidant (air).

Functionalized samples were coded with the acronym PPAA_Xy_Z, where X indicates the post-deposition treatments (namely: W for water incubated, WT for the water incubated/thermally treated and 0 for untreated samples), y indicates the analyzed mesh-side (i.e. front=a and back=b, if applicable) and Z indicates the aging storage atmosphere (namely: N for 3 months aged samples stored in nitrogen, A for 3 months aged samples stored in air and 0 for non-stored as-functionalized samples). Original PP non-functionalized mesh was taken as reference material and coded as Ref.

2.3 TBO titration and quantification of carboxylic functionalities density

The amount of -COOH functionalities of PPAA was tested with Toluidine Blue O (TBO) colorimetric determination. The amino group contained in TBO molecule reacts specifically with a surface carboxylic group according to a 1:1 ratio [24]. PPAA-functionalized samples were contacted with 3 mL of 0.5 mM TBO aqueous solution (pH = 10) at 37 °C, for 5 h, in the dark. To remove the unreacted dye, meshes were rinsed with copious amount of 0.1 mM NaOH solution. Afterwards, samples were transferred in 1.5 ml of 50 % v/v acetic acid solution and shaken for 10 minutes, in order to completely release the TBO linked to the carboxylic functional groups. Colorimetric dosing of TBO (and consequently of carboxylic groups) was performed by using a double beam UV-Vis-NIR Varian Cary 5000 spectrophotometer, in transmission mode. All the spectra were obtained by using a quartz cuvette and monitoring the λ_{max} = 633 nm. A solution of 50 % v/v acetic acid was used as reference background. The experiments were repeated twice. The evaluation of carboxylic functionalities density (in terms of groups cm^{-2} of mesh) was performed through the Lambert-Beer law on the basis of an external calibration with TBO solutions (at known concentrations and volumes) and a multiplex replication of experimental values. Finally, the -COOH amount was normalized for the geometric surface of mesh samples used for the analysis (i.e. 4 cm^2). External calibration curve is reported in **Figure S1**.

2.4 Physicochemical characterization techniques

Static (sessile drop) water contact angle (WCA) measurements were performed by using OCAH200 (Dataphysics, Instruments GmbH). 1.5 µL of dH_2O was spotted onto the meshes surfaces at Room Temperature (RT) and images of the droplets were captured. SCA20 software was used to fit drop profiles through the Young-Laplace method and, indeed, to calculate contact angles between fitted function and baseline. The instrument automatically calculates the contact angle, allowing to roughly estimate the hydrophilic/hydrophobic behavior of the material surface. At least three drops were dispensed for each sample.

Fourier Transform Infrared Spectra (FTIR) spectra were recorded in Attenuated Total Reflection mode (ATR, using a diamond cell for single reflection) in a Bruker Vector 22 spectrophotometer equipped with Globar source, DTGS detector and working with 128 scans at 4 cm^{-1} of resolution in the range 4000-400 cm^{-1}. ATR-FTIR spectra were obtained on single fibers repeating the acquisition for three times.

X-ray Photoemission Spectroscopy (XPS) studies were carried out by a Versa Probe 5000 from PHI electronics, using Summit as software. Spectra were analyzed using Fityk software. Al Kα radiation (1486.6 eV), having a beam diameter of 100 µm, was used as X-ray source. C1s and O1s (not discussed) signals were analyzed. All core-level peak energies were referenced to C1s peak at 284.5 eV assignable to the surface accumulated adventitious carbon.

The adhesive properties of the PPAA-functionalized biomaterials were evaluated by Atomic Force Microscopy (AFM) in Force/Distance mode to measure adhesion forces between the AFM probe and the PPAA coating. Analyses were performed in air at RT with a Park Systems Instrument, model XE-100. Silicon microcantilevers with the reflective side coated with aluminum (force constant 3.0 N m^{-1}, frequency constant 60 kHz) and tetrahedral silicon tip (radius of curvature less than 8 nm, tip height 20-25 µm, full tip cone angle less than 30°) were used. Probe dimensions were 200 µm length, 40 µm wide and 2 µm thick. The cantilever loading/unloading speed was 0.15 µm s^{-1}. The F/D plot reports the force existing between the tip and the sample as a function of the Z scanner extension. Adhesion forces were calculated as the unloading force change at the minimum value of the loading force. To calibrate tips force, measurements were done on a glass surface previously cleaned with acetone solution and then heated up in an oven at 100 °C for 1 hours and cooled down to RT. All adhesion force measurements were performed more than 10 times on the functionalized meshes along the fibers/knots and average values were reported with their standard deviations.

3. Results and Discussion

3.1 Plasma-induced surface fuctionalization at the PP surface

After the deposition treatments, the PPAA-functionalized PP meshes were divided in three groups according to the different applied post-deposition conditions: i) untreated PPAA-functionalized samples; ii) incubated PPAA-functionalized samples (i.e. soaked in deionized water Milli-Q grade for 30 minutes under oscillating shaking), and iii) incubated and thermally treated PPAA-functionalized samples (i.e. incubated samples were dried under N_2 flux and heated at 80 °C for 1 hour in oven).

Immediately after the plasma polymerization treatment (i.e. within 30 min), the surface wettability/hydrophilicity of functionalized devices was evaluated by means of water contact angle (WCA) measurements (numerical data are reported in **Table 1**). **Figure 1** shows a reduction of contact angle values, from ca. 140° for untreated reference fibers (section A) to ca. 42° for PPAA-functionalized ones (section B), which corresponds to the increase of the surface hydrophilicity. On the contrary, the post-deposition treatments caused a controlled reduction of wettability as shown by WCA change to ca. 116° for incubated PPAA-samples (section C) and ca. 110° for incubated/thermally treated ones (section D). Fibers hydrophilicity variations seems to be proportionally related to the efficiency of mesh functionalization (i.e. the presence and surface density of carboxylic functionalities due to PPAA coatings). Additionally, as reported in our previous work [23], it is not easy to distinguish any morphological variations due to PPAA functionalization on PP fibers, probably for the limited thickness of the coating (ca. 100 ± 20 nm). However, after plasma-induced PPAA functionalization, PP surface appears smooth and without irregularities (see **Figure S2**), thus any contact angle decrease can be attributed only to surface chemistry modifications.

The presence of the PPAA coating in the functionalized samples was confirmed through Infrared Spectroscopy (FTIR) measurements by the presence of the signals typical of reference PolyAcrylic Acid (PAA) material (3500-3000 cm^{-1} due to the hydroxyl -OH single bond stretching, and at 1720 cm^{-1} due to the carbonyl C=O double bond stretching of carboxylic acids [23]). Infrared spectra were collected in ATR mode on PP fibers before and after PPAA-functionalization, after post-deposition treatments and the relevant curves are reported in **Figure 2**. All spectra confirm the presence of PAA. Furthermore, ATR-FTIR measurements were also performed on both sides of functionalized meshes (front and back) in order to check the effectiveness of the plasma-induced deposition on the mesh back side not-directly exposed to the acrylic acid vapors containing reactive atmosphere. Incubated samples (namely W and WT curves) present the PPAA-functionalities only on the mesh-side directly exposed to the monomer vapors, whereas the PPAA-functionalized not-treated meshes show the PAA typical signals on both sides. As reported in the literature [13], water washing can remove the oligomeric components formed during the plasma polymerization. The

absence of the PAA signals on the meshes after incubation (and incubation/thermal treatment) indicates that, on the back side of the meshes, only oligomeric species are formed probably as by-products of direct polymerization reactions occurring on the front size and randomly transported on the back size by the gaseous mixture flow.

The carboxylic functionalities surface density on the coated prostheses was determined by means of TBO colorimetric titration. The procedure was applied to both untreated reference PP fibers and PPAA-functionalized fibers subjected to all the post-deposition treatments (numerical data are reported in **Table 1**).

Results collected in **Figure 3** indicate that the PPAA-functionalized meshes present a remarkable amount of carboxylic functional groups per unit area (geometric surface of analyzed mesh = 4 cm^2). As already predicted by WCA and FTIR analyses, PPAA-functionalized untreated meshes possess a great amount of carboxylic units, supposed to derive mainly from oligomers presence. Indeed, it is interesting to note that -COOH amount revealed by TBO assay is high although oligomers should be washed away during the 5-hours soaking in TBO solution. This suggests that -COOH groups are stably bonded at the surface of the meshes probably because oligomers continue to polymerize and/or cross-link after the deposition transforming in a more stably bonded coating. Actually, it is well-known the potential latent reactivity of metastable radicals present in plasma-polymerized polymers, even after the end of the plasma-process. Finally, reference PP meshes present a small but not negligible amount of carboxylic groups. Their presence can be related to a certain degree of surface oxidation (producing -COOH groups) or to some TBO strong surface physisorption due to fibers surface porosity.

X-ray Photoemission Spectroscopy (XPS) measurements were carried out and data collected in **Figure 4**. Only the main signals due to C1s and evident intensity ratio changes will be thoroughly discussed. Variations in the single component intensity will be not discussed since differences even limited in the coating thickness can affect this behavior. Untreated PP fibers present the main component due to C-C/C-H species and a very weak C-O signal due to a limited surface oxidation that confirms the TBO titration data. In accordance with WCA and TBO measurements, untreated PPAA-functionalized samples show the formation of oxygen-containing functional groups (C-O and HO-C=O) whereas post-deposition treatments cause the lack of part of the oxygenated surface groups. An interesting feature is evidenced by the spectrum of the incubated/thermally treated sample: an evident broadening of the C-C/C-H peak and a shift towards higher energies of the C-O signal is observed, indicating a possible modification of the outer layer of the sample. Nevertheless HO-C=O signal remains almost stable confirming the thermal stability of the coating.

3.2 PPAA-functionalized meshes: Effect due to aging conditions

PPAA-functionalized samples were 3 months aged under two different storage atmospheres: inert (nitrogen) and humid/oxidant (air). WCA measurements carried out onto PPAA-functionalized meshes 3 months aged (see **Figure 5**) indicate two different effects depending on the starting samples and their understanding is not trivial. In fact, as reported in **Table 1**, untreated samples after aging (PPAA_0_Z) present a decrease of the WCA which becomes not-detectable, independently from the aging atmosphere so indicating an increase of the hydrophilicity of the sample. As already evidenced by the FTIR analysis of the untreated samples (**Figure 2**), AA oligomers can organize themselves in order to expose the largest number of -COOH functionalities far from the hydrophobic PP support. This rearrangement should be responsible of the increase the coating hydrophilicity. Contact angles of incubated samples (PPAA_W_Z) appear to be slightly higher after aging in air, thus suggesting a partial hydrophobization of the surface, probably due to the reactivity and consequent loss of -COOH groups exposed to the air (see **Table 1**), whereas no effects are visible after aging in nitrogen which seems to preserve the -COOH groups. No significant effects are visible for incubated/thermally treated samples after aging in both atmospheres.

The signal intensities of carbonyl FTIR absorption at 1720 cm^{-1} were evaluated and average values for PPAA-functionalized fibers before and after 3 months of aging in inert (nitrogen) or

humid/oxidant (air) atmospheres were reported in **Table S1**, in order to confirm this behavior, the results support that PPAA coatings are still present after 3 months of aging, independently from the aging atmosphere. The same conclusion can be achieved considering the front and back sides of non-incubated meshes.

As reported in **Figure 3** (and in **Table 1**), it has been confirmed that samples overcoming post-deposition treatments present similar carboxylic groups density values, thus indicating that the aging under different atmospheres does not modify significantly the effect of post-deposition treatments. Additionally, it is interesting to notice that the degradation of unstable species is particularly discouraged for meshes stored under nitrogen (i.e. inert atmosphere), since the cross-linking is more efficient and favored.

XPS measurements concerning aged samples are collected in **Figure 6**. Basing on obtained results, different modifications were achieved depending on the applied post-deposition treatment. The C1s signals related to PPAA-functionalized samples incubated (even thermally treated) and aged in both atmospheres (C-E) are not significantly different with respect to the data reported in **Figure 4**. Conversely, untreated PPAA-functionalized samples (A, B) show a decrease of the C-O component and the sample aged in nitrogen (A) exhibits the growth of a new component at 282.2 eV, probably due to oligomers degradation products or to secondary species formed by oligomers still reacting after the deposition. The formation of these unknown products could affect the behaviors of the meshes in an uncontrolled, even negative, manner so suggesting that a post-deposition treatment could be recommended. However, the application of a thermal treatment at 80 °C after the incubation step is detrimental due to the probable increase of PPAA layer reactivity , since a very small component at 282.2 eV is as well revealed by XPS measurements (F). This behavior suggests to avoid the thermal treatment and to perform the post-deposition treatment only by water washing.

3.3 Adhesive properties evaluation by AFM in F/D mode

Adhesive properties of meshes before and after the PPAA-functionalization (and aging) were evaluated by means of AFM F/D measurements. This technique allows the measurement of surface weak forces and provides information on surface energetic behaviors of materials [21]. In this particular context, AFM in F/D mode allows to directly measure the adhesion forces between the AFM probe tip and prosthetic meshes (neat and PPAA-functionalized, before and after post-deposition treatments and/or aging). Obviously this technique provides the interaction between the adhesive coating and a silicon tip (thus not to body tissues), therefore it cannot be used as a direct substituting assay of *in vitro* tests. However, the real powerfulness of such method is the reliable mapping of the surface, giving a statistical behavior in terms of homogeneity of the adhesive coating towards the cylindrical fibers forming the prosthetic device as well as a measurement of the relative adhesive force compared to the neat PP sample. As reported in the literature, several parameters can influence the adhesion forces measured through AFM in F/D mode, but the main relevant ones are two: i) surface roughness, and ii) hydrogen and van der Waals interactions [25-32]. However, as previously discussed, negligible morphological variations in the fibers are evidenced after plasma treatment (**Figure S2**). Additionally, PPAA-functionalized PP fibers present smooth surfaces without irregularities (thus avoiding any mechanical-induced factor affecting the measured adhesion forces).

Adhesion forces measured by AFM in F/D mode are presented in **Figure 7** in form of histograms, whereas numerical data are reported in **Table 1**.

In general, adhesion forces exerted by PPAA-functionalized meshes toward the silicon probe tip are significantly higher (namely twice or even more) than the reference standard PP material (i.e. 8.5 ± 0.8 nN is measured for Ref sample). Untreated PPAA-functionalized samples exert adhesion forces higher than the post-deposition treated PPAA-functionalized samples (the relative values are 28.5 ± 2.6 nN for PPAA_0_0, 15.5 ± 1.5 nN for PPAA_W_0 and 15.5 ± 3.1 nN for PPAA_WT_0), as expected considering the previously discussed data. These data are in agreement with the consideration obtained by using WCA, FTIR and TBO analysis.

The aging of post-deposition treated samples does not seem to have significantly altered the PPAA coating, since no significant change of the adhesive properties is observed, whatever the storage atmosphere applied. On the contrary, the storage of untreated meshes causes important inhomogeneity in the adhesive properties as witnessed by the standard deviation, which reaches the maximum value for samples stored in nitrogen. Again, the uncontrolled reactivity of the AA oligomers seems to be responsible of this particular behavior.

4. Conclusions

This paper deals with the plasma-induced polymerization of acrylic acid vapors onto PP hernia-repair prostheses and the evaluation of such adhesive coating stability and aging. A broad physicochemical characterization has been carried out, so confirming the presence of the PPAA coating and assessing the amount of carboxyl functionality density at the biomaterials surface. AFM in F/D mode assessed itself as a real powerful tool for evaluating the adhesion capability of such PPAA-functionalized devices.

Once PP meshes were functionalized, different post-deposition treatments (i.e. incubation, or incubation/thermal treatment) were investigated, with the aim of monitoring the coating degradation (and therefore the loss of adhesion) after 3 months of aging in both inert (nitrogen) and humid/oxidant (air) atmospheres.

On the basis of obtained results, it is possible to conclude that a post-deposition treatment (for instance a water washing) is mandatory in order to remove all the unstable and reactive oligomers produced during the plasma-treatment at the PP surface. No significant variations in terms of both physicochemical and adhesion properties were registered for incubated PPAA-functionalized meshes after 3 months of aging under different storage atmospheres, so indicating that these devices can be simply stored in presence of air for at least three months without a meaningful degradation of the original properties.

In conclusion, plasma-polymerization is assessed to be a convenient procedure for the surface modification of polymeric biomaterials by means of the deposition of a conformal and stable thin coating, durable in time, even if thermally treated at 80°C. Additionally, by means of AFM in F/D mode it was possible to directly evaluate the coating homogeneity and stability along the PP fibers, to confirm the importance of a post-deposition treatment and evaluate the best storage conditions for making these functional devices truly industrially-applicable.

5. Acknowledgements

The authors would like to thank Dr. Salvatore Guastella (from Politecnico di Torino, DISAT, Italy) for XPS measurements.

References

[1] B. Klosterhalfen, K. Junge, U. Klinge, The lightweight and large porous mesh concept for hernia repair, **Expert Review of Medical Devices** 2 (2005) 103-117.

[2] B. Klosterhalfen, U. Klinge, V. Schumpelick, Functional and morphological evaluation of different polypropylene-mesh modifications for abdominal wall repair, **Biomaterials** 19 (1998) 2235-2246.

[3] A. Coda, R. Lamberti, S. Martorana, Classification of prosthetics used in hernia repair based on weight and biomaterial, **Hernia** 16 (2012) 9-20.

[4] J.R. DeBord, The historical development of prosthetics in hernia surgery, **Surgical Clinics of North America** 78 (1998) 973-1006.

[5] P.K. Amid, Classification of biomaterials and their related complications in abdominal wall hernia surgery, **Hernia** 1 (1997) 15-21.

[6] P.K. Chu, J.Y Chen, L.P. Wang, N. Huang, Plasma-surface modification of biomaterials, **Materials Science and Engineering R: Reports** 36 (2002) 143-206.

[7] N.Y. Cui, N.M.D. Brown, Modification of the surface properties of a polypropylene (PP) film using an air dielectric barrier discharge plasma, **Applied Surface Science** 189 (2002) 31-38.
[8] J. Lai, B. Sunderland, J. Xue, S. Yan, W. Zhao, M. Folkard, B.D. Michael, Y. Wang, Study on hydrophilicity of polymer surfaces improved by plasma treatment, **Applied Surface Science** 252 (2006) 3375-3379.
[9] R. Nisticò, G. Magnacca, M.G. Faga, G. Gautier, D. D'Angelo, E. Ciancio, R. Lamberti, S. Martorana, Effect of atmospheric oxidative plasma treatments on polypropylenic fibers surface: characterization and reaction mechanisms, **Applied Surface Science** 279 (2013) 285-292.
[10] R. Forch, Z.H. Zhang, W. Knoll, Soft plasma treated surfaces: tailoring of structure and properties for biomaterial applications, **Plasma Processes and Polymers** 2 (2005) 351-372.
[11] R. Nisticò, M.G. Faga, G. Gautier, G. Magnacca, D. D'Angelo, E. Ciancio, G. Piacenza, R. Lamberti, S. Martorana, Physico-chemical characterization of functionalized polypropylenic fibers for prosthetic applications, **Applied Surface Science** 258 (2012) 7889-7896.
[12] P. Avetta, R. Nisticò, M.G. Faga, D. D'Angelo, E. Aimo Boot, R. Lamberti, S. Martorana, P. Calza, D. Fabbri, G. Magnacca, Hernia-repair prosthetic devices functionalised with chitosan and ciprofloxacin coating: controlled release and antibacterial activity, **Journal of Materials Chemistry B** 2 (2014) 5287-5294.
[13] S. Ricciardi, R. Castagna, S.M. Severino, I. Ferrante, F. Frascella, E. Celasco, P.Mandracci, I. Vallini, G. Mantero, C.F. Pirri, P. Rivolo, Surface functionalization by poly-acrylic acid plasma-polymerized films for microarray DNA diagnostics, **Surface and Coatings Technology** 207 (2012) 389-399.
[14] J.H. Lee, J.W. Lee, G. Khang, H.B. Lee, Interaction of cells on chargeable functional group gradient surfaces, **Biomaterials** 18 (1997) 351-358.
[15] L. Detomaso, R. Gristina, G.S. Senesi, R. d'Agostino, P. Favia, Stable plasma deposited acrylic acid surfaces for cell culture applications, **Biomaterials** 26 (2005) 3831-3841.
[16] H. Yasuda, T. Hirotsu, Critical evaluation of conditions of plasma polymerization, **Journal of Polymer Science: Polymer Chemistry Edition** 16 (1978) 743-759.
[17] H. Yasuda, *Luminous Chemical Vapor Deposition and Interface Engineering*, Marcel Dekker, New York (New York, USA), 2004.
[18] D. Hegemann, M.M. Hossain, E. Körner, D.J. Balazs, Macroscopic description of plasma polymerization, **Plasma Processes and Polymers** 4 (2007) 229-238.
[19] C. Corbella, I. Bialuch, M. Kleinschmidt, K. Bewilogua, Up-scaling the production of modified a-C:H coatings in the framework of plasma polymerization processes, **Solid State Sciences** 11 (2009) 1768-1772.
[20] M.C.M. van de Sandem, Views on macroscopic kinetics of plasma polymerization: Acrylic acid revisited, **Plasma Processes and Polymers** 7 (2010) 887-888.
[21] H.J. Lee, S. Hyun, J.H. Kim, H.J. Lee, D.G. Choi, D.I. Lee, J.H. Jeong, E.S. Lee, Measurement of adhesion force by a symmetric AFM probe for nano-imprint lithography application, **Journal of Adhesion Science and Technology** 22 (2008) 1379-1386.
[22] B. Cappella, G. Dietler, Force-distance curves by atomic force microscopy, **Surface Science Reports** 34 (1999) 1-3, 5-104.
[23] R. Nisticò, A. Rosellini, P. Rivolo, M.G. Faga, R. Lamberti, S. Martorana, M. Castellino, A. Virga, P. Mandracci, M. Malandrino, G. Magnacca, Surface functionalisation of polypropylene hernia-repair meshes by RF-activated plasma polymerisation of acrylic acid and silver nanoparticles, **Applied Surface Science** 328 (2015) 287-295.
[24] J.P. Chen, Y.P. Chiang, Surface modification of non-woven fabric by DC pulsed plasma treatment and graft polymerization with acrylic acid, **Journal of Membrane Science** 270 (2006) 212-220
[25] I.M. Pelin, A. Piednoir, D. Machon, P. Farge, C. Pirat, S.M.M. Ramos, Adhesion forces between AFM tips and superficial dentin surfaces**, Journal of Colloid and Interface Science** 376 (2012) 262-268.

[26] J.R. Smith, J. Tsibouklis, T.G. Nevell, S. Breakspear, AFM friction and adhesion mapping of the substructures of human hair cuticles, **Applied Surface Science** 285 B (2013) 638-644.
[27] M. Huson, D. Evans, J. Church, S. Hutchinson, J. Maxwell, G. Corino, New insights into the nature of the wool fibre surface, **Journal of Structural Biology** 163 (2008) 127-136.
[28] G. Raj, E. Balnois, C. Baley, Y. Grohens, Role of polysaccharides on mechanical and adhesion properties of Flax fibres in Flax/PLA biocomposite, **International Journal of Polymer Science** 2011 (2011) Article ID 503940.
[29] G. Raj, E. Balnoiso, C. Baley, Y. Grohens, Adhesion force mapping of raw and treated flax fibres using afm force-volume, **Journal of Scanning Probe Microscopy** 4 (2009) 66-72.
[30] O. Dos Santos Ferreira, E. Gelinck, D. de Graaf, H. Fischer, Adhesion experiments using an AFM-Parameters of influence, **Applied Surface Science** 257 (2010) 48-55.
[31] H.J. Butt, B. Cappella, M. Kappl, Force measurements with the atomic force microscope: technique, interpretation and applications, **Surface Science Reports** 59 (2005) 1-152.
[32] R. Jones, H.M. Pollock, J.A.S. Cleaver, C.S. Hodges, Adhesion forces between glass and silicon surfaces in air studied by AFM: effects of relative humidity, particle size, roughness, and surface treatment, **Langmuir** 18 (2002) 8045-8055.

Caption to Figures

Table 1. Average WCA values, carboxyl functionality density and adhesion force evaluated for untreated PP meshes and PPAA-functionalized samples.

Figure 1. WCA observed for untreated reference PP fibers (A), PPAA-functionalized untreated fibers (B), PPAA-functionalized fibers incubated (C) and PPAA-functionalized fibers incubated/thermally treated (D).

Figure 2. Absorbance IR spectra in the 4000-2400 cm^{-1} range and in the 1900-500 cm^{-1} range relative to untreated reference PP fibers (Ref), PPAA-functionalized untreated fibers (0), PPAA-functionalized fibers incubated (W), PPAA-functionalized fibers incubated/thermally treated (WT) and commercial PAA film (PAA, black dotted line). Comparison between front (black solid lines) and back (grey solid lines) sides. Commercial PAA film spectrum was collected in transmission mode, whereas the fibers spectra were collected in ATR mode.

Figure 3. Carboxyl functionality density evaluated for untreated reference PP fibers (Ref, white block), PPAA-functionalized untreated fibers (PPAA_0_Z, horizontally-striped blocks), PPAA-functionalized fibers incubated (PPAA_W_Z, oblique-striped blocks) and PPAA-functionalized fibers incubated/thermally treated (PPAA_WT_Z, cross-striped blocks). For each post-deposition treatment, the first block represents the PPAA-functionalized meshes (PPAA_X_0), the second and the third blocks represent the values after 3 months of aging under nitrogen (PPAA_X_N) and air (PPAA_X_A) respectively. Average values were obtained repeating the acquisition twice.

Figure 4. XPS spectra of untreated reference PP fibers (A), PPAA-functionalized untreated fibers (B), PPAA-functionalized fibers, incubated (C) and PPAA-functionalized fibers, incubated/thermally treated (D). C1s signals: experimental curve (black solid line), fit curve (black dashed line), C–C/C–H signal at 284.5 eV (grey solid line), C–O signal in the range 286.6-285.6 eV (grey dashed line) and HO–C=O signal at 288.6 eV (grey dotted line).

Figure 5. WCA observed for PPAA-functionalized untreated fibers aged in nitrogen (A) and in air (B), PPAA-functionalized fibers incubated and aged in nitrogen (C) and in air (D), PPAA-functionalized fibers incubated/thermally treated and aged in nitrogen (E) and in air (F).

Figure 6. XPS spectra of PPAA-functionalized untreated fibers aged in nitrogen (A) and in air (B), PPAA-functionalized fibers, incubated and aged in nitrogen (C) and in air (D), PPAA-functionalized fibers, incubated/thermally treated and aged in nitrogen (E) and in air (F). C1s signals: experimental curve (black solid line), fit curve (black dashed line), C–C/C–H signal at 284.5 eV (grey solid line), C–O signal in the range 286.6-285.6 eV (grey dashed line), HO–C=O signal at 288.6 eV (grey dotted line) and an extra-unknown component C–X at 282.2 eV (black dotted line).

Figure 7. Adhesion force evaluated for untreated reference PP fibers (Ref, white block), PPAA-functionalized untreated fibers (PPAA_0_Z, horizontally-striped blocks), PPAA-functionalized fibers incubated (PPAA_W_Z, oblique-striped blocks) and PPAA-functionalized fibers incubated/thermally treated (PPAA_WT_Z, cross-striped blocks). For each post-deposition treatment, the first block represents the PPAA-functionalized meshes (PPAA_X_0), the second and the third blocks represent the value after 3 months of aging under nitrogen (PPAA_X_N) and air (PPAA_X_A) respectively. Average values were obtained repeating the acquisition for 10 times.

Table 1. Average WCA values, carboxyl functionality density and adhesion force evaluated for untreated PP meshes and PPAA-functionalized samples.

Samples name	WCA[a]	Carboxyl functionality density[b]	Adhesion force[c]
Ref	139 ± 1	$(3.145 \pm 1.601) \times 10^{14}$	8.5 ± 0.8
PPAA_0_0	42 ± 13	$(4.550 \pm 0.945) \times 10^{15}$	28.5 ± 2.6
PPAA_0_N	n.d. (< 5)	$(8.355 \pm 0.043) \times 10^{15}$	40.4 ± 10.9
PPAA_0_A	n.d. (< 5)	$(4.414 \pm 1.164) \times 10^{15}$	26.7 ± 3.9
PPAA_W_0	116 ± 6	$(2.086 \pm 0.074) \times 10^{15}$	15.5 ± 1.5
PPAA_W_N	118 ± 1	$(2.766 \pm 0.201) \times 10^{15}$	16.0 ± 0.8
PPAA_W_A	134 ± 11	$(2.061 \pm 0.099) \times 10^{15}$	20.3 ± 3.1
PPAA_WT_0	110 ± 7	$(2.697 \pm 0.221) \times 10^{15}$	15.5 ± 3.1
PPAA_WT_N	119 ± 9	$(3.423 \pm 1.207) \times 10^{15}$	20.2 ± 2.9
PPAA_WT_A	113 ± 7	$(2.182 \pm 0.198) \times 10^{15}$	16.0 ± 2.5

[a] WCA values are reported as degrees (°) ± SD (or Standard Deviation).

[b] Carboxyl functionality densities are reported in number of -COOH groups per cm^2 of mesh ± SD (or Standard Deviation).

[c] Adhesion forces are reported in nN ± SD (or Standard Deviation).

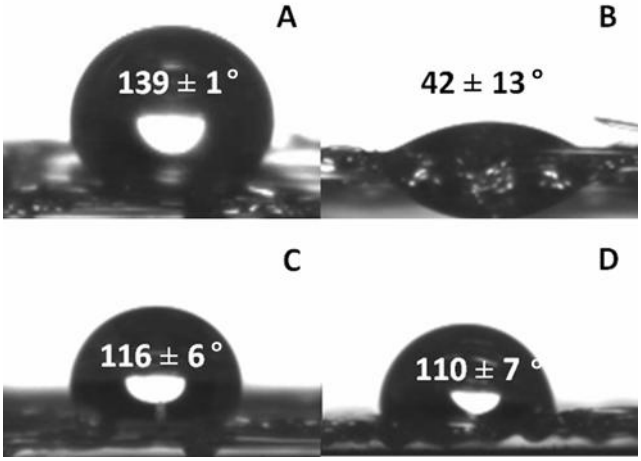

Figure 1. WCA observed for untreated reference PP fibers (A), PPAA-functionalized untreated fibers (B), PPAA-functionalized fibers incubated (C) and PPAA-functionalized fibers incubated/thermally treated (D).

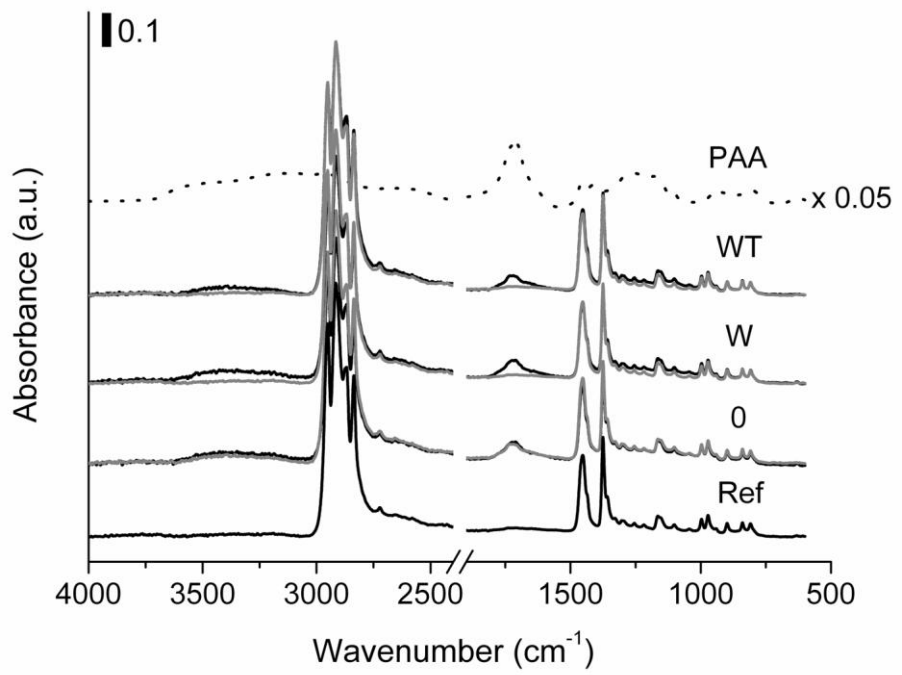

Figure 2. Absorbance IR spectra in the 4000-2400 cm^{-1} range and in the 1900-500 cm^{-1} range relative to untreated reference PP fibers (Ref), PPAA-functionalized untreated fibers (0), PPAA-functionalized fibers incubated (W), PPAA-functionalized fibers incubated/thermally treated (WT) and commercial PAA film (PAA, black dotted line). Comparison between front (black solid lines) and back (grey solid lines) sides. Commercial PAA film spectrum was collected in transmission mode, whereas the fibers spectra were collected in ATR mode.

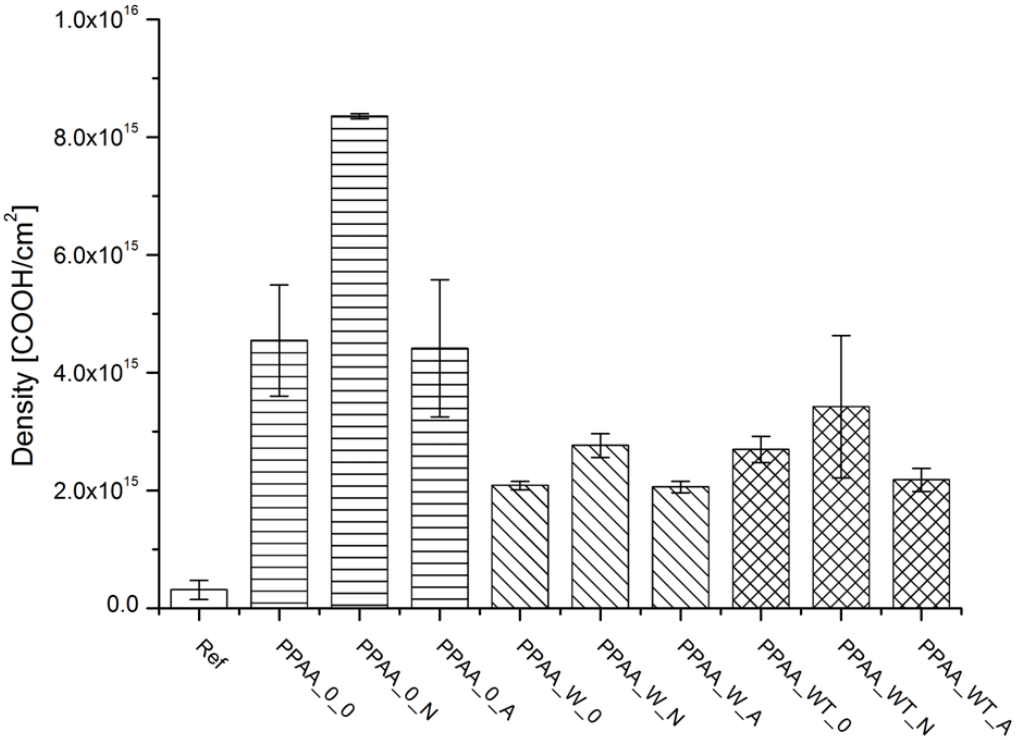

Figure 3. Carboxyl functionality density evaluated for untreated reference PP fibers (Ref, white block), PPAA-functionalized untreated fibers (PPAA_0_Z, horizontally-striped blocks), PPAA-functionalized fibers incubated (PPAA_W_Z, oblique-striped blocks) and PPAA-functionalized fibers incubated/thermally treated (PPAA_WT_Z, cross-striped blocks). For each post-deposition treatment, the first block represents the PPAA-functionalized meshes (PPAA_X_0), the second and the third blocks represent the values after 3 months of aging under nitrogen (PPAA_X_N) and air (PPAA_X_A) respectively. Average values were obtained repeating the acquisition twice.

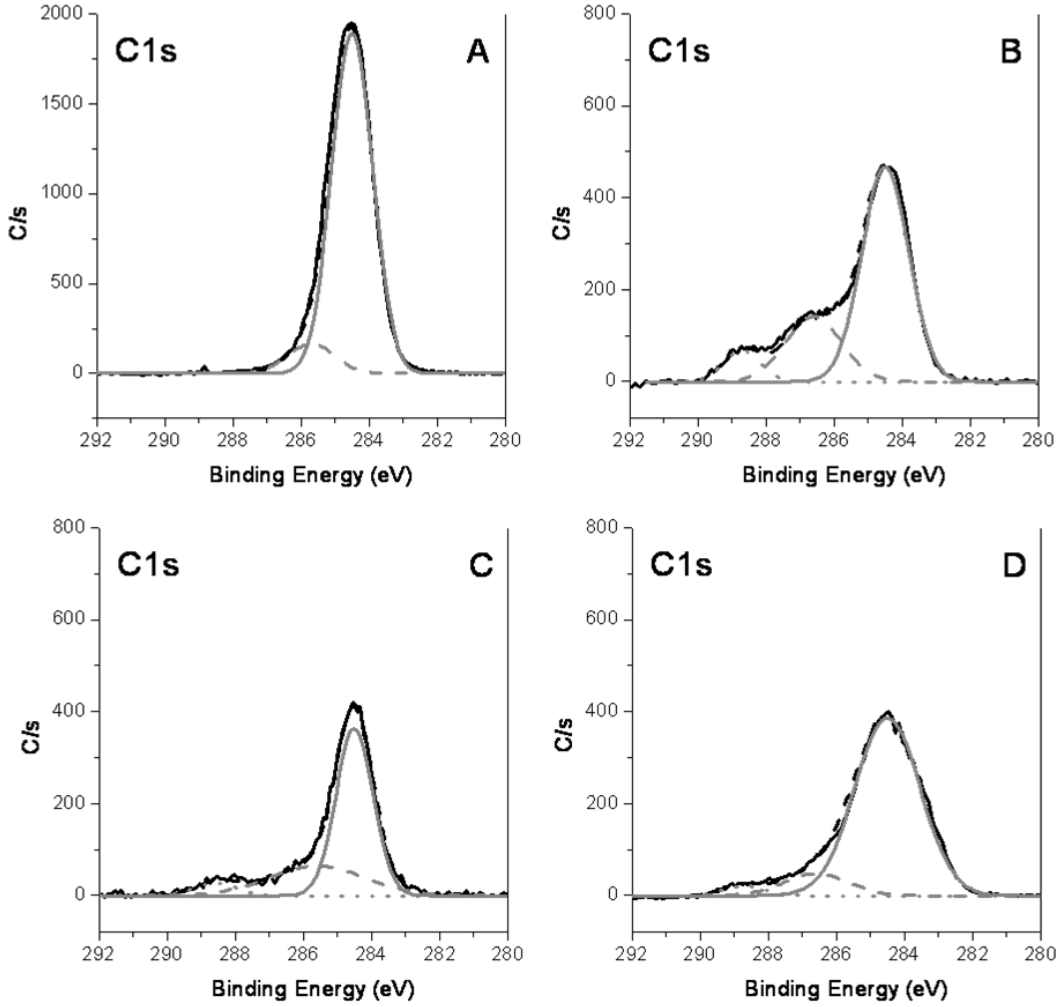

Figure 4. XPS spectra of untreated reference PP fibers (A), PPAA-functionalized untreated fibers (B), PPAA-functionalized fibers, incubated (C) and PPAA-functionalized fibers, incubated/thermally treated (D). C1s signals: experimental curve (black solid line), fit curve (black dashed line), C–C/C–H signal at 284.5 eV (grey solid line), C–O signal in the range 286.6-285.6 eV (grey dashed line) and HO–C=O signal at 288.6 eV (grey dotted line).

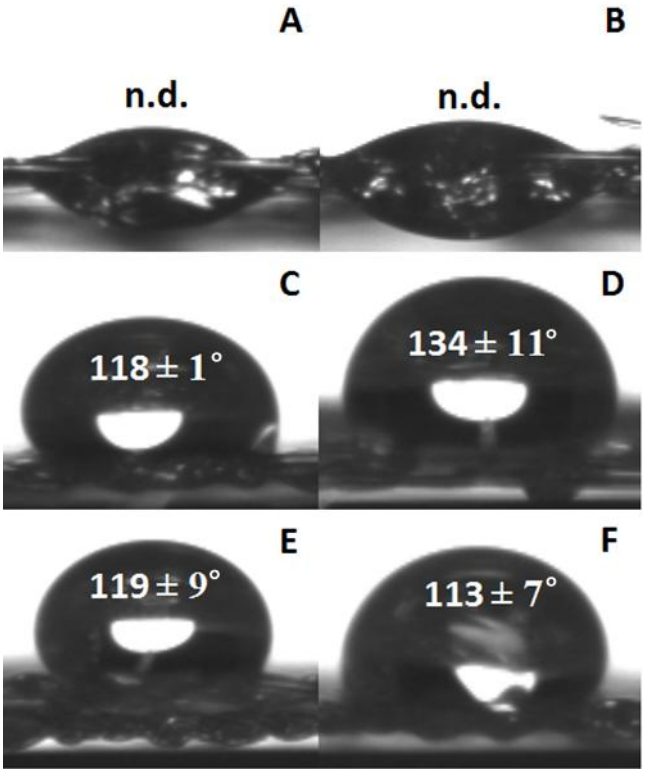

Figure 5. WCA observed for PPAA-functionalized untreated fibers aged in nitrogen (A) and in air (B), PPAA-functionalized fibers incubated and aged in nitrogen (C) and in air (D), PPAA-functionalized fibers incubated/thermally treated and aged in nitrogen (E) and in air (F).

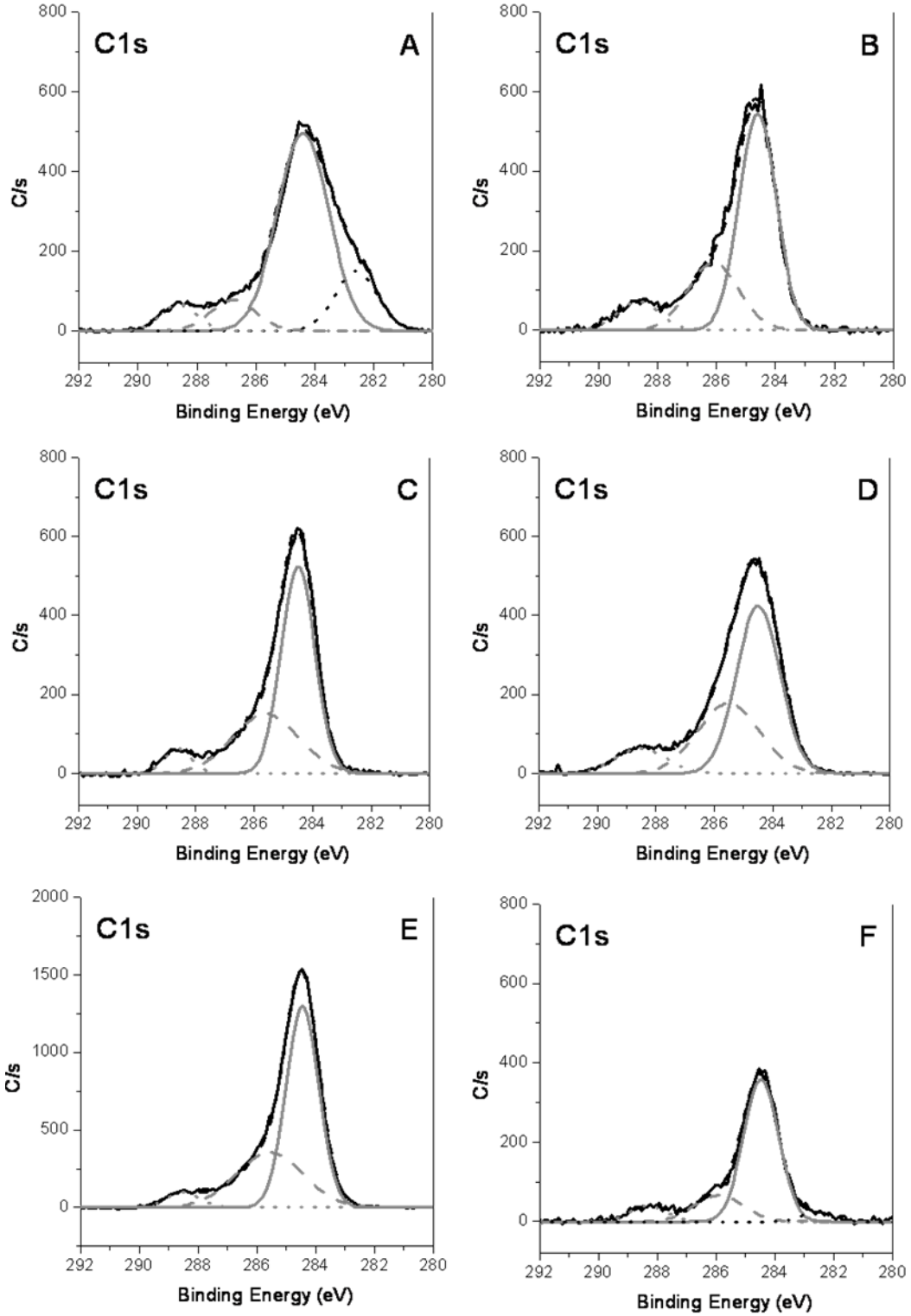

Figure 6. XPS spectra of PPAA-functionalized untreated fibers aged in nitrogen (A) and in air (B), PPAA-functionalized fibers, incubated and aged in nitrogen (C) and in air (D), PPAA-functionalized fibers, incubated/thermally treated and aged in nitrogen (E) and in air (F). C1s signals: experimental curve (black solid line), fit curve (black dashed line), C–C/C–H signal at 284.5 eV (grey solid line), C–O signal in the range 286.6-285.6 eV (grey dashed line), HO–C=O signal at 288.6 eV (grey dotted line) and an extra-unknown component C–X at 282.2 eV (black dotted line).

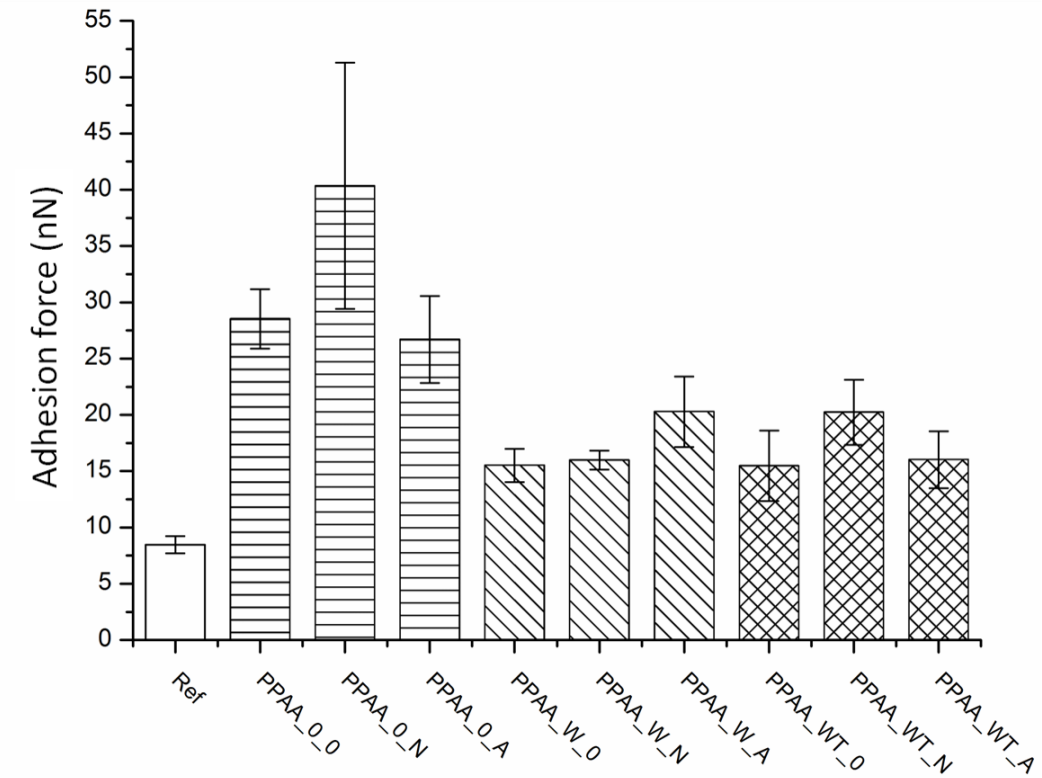

Figure 7. Adhesion force evaluated for untreated reference PP fibers (Ref, white block), PPAA-functionalized untreated fibers (PPAA_0_Z, horizontally-striped blocks), PPAA-functionalized fibers incubated (PPAA_W_Z, oblique-striped blocks) and PPAA-functionalized fibers incubated/thermally treated (PPAA_WT_Z, cross-striped blocks). For each post-deposition treatment, the first block represents the PPAA-functionalized meshes (PPAA_X_0), the second and the third blocks represent the value after 3 months of aging under nitrogen (PPAA_X_N) and air (PPAA_X_A) respectively. Average values were obtained repeating the acquisition for 10 times.